Continuous Flow vs. Static Chamber μPCR Devices on Flexible Polymeric Substrates

Vasileios E. PAPADOPOULOS, Ioanna N. KEFALA, George KOKKORIS*, and Angeliki TSEREPI*

*Corresponding authors: Tel.: ++30 2106503238; Fax: ++30 210 6511723; Email: gkok@imel.demokritos.gr, atserepi@imel.demokritos.gr
Institute of Nanoscience and Nanotechnology, NCSR "Demokritos", Greece

Abstract Two types of μPCR devices, a continuous flow and a static chamber device, fabricated on flexible polymeric substrates are compared in the current computational study. Laminar flow, heat transfer in both solid and fluid, mass conservation of species, and reaction kinetics of PCR are coupled using COMSOL. The comparison is performed under same conditions; same material stack (based on flexible polymeric films with integrated microheaters), same species initial concentrations, amplification of the same volume of fluid sample, and implementation of the same PCR protocol. Performance is quantified in terms of DNA amplification, energy consumption, and total operating time. The calculations show that the efficiency of DNA amplification is higher in the continuous flow device. However, the continuous flow device requires (~6 times) greater energy consumption which is justified by the smaller thermal mass of the static chamber device. As regards the speed, the total time required for the static chamber μPCR is comparable to the time for the continuous flow μPCR.

Keywords: microflow, heat transfer, PCR, microfluidics, DNA amplification, continuous flow, static chamber, μTAS, LoC, flexible substrates

1. Introduction

Polymerase chain reaction (PCR) can create copies of specific fragments of DNA by thermal cycling (Kumar et al., 2008). A typical PCR includes denaturation of double-stranded DNA (at 95^{o}C), annealing of primers (at 55^{o}C), and extension of the primer-bound sequences (at 72^{o}C). Each thermal cycle can double the amount of DNA, and 20–35 cycles can produce millions of DNA copies.

Miniaturized or micro-PCR (μPCR) devices can be categorized into static chamber and continuous flow devices. The static chamber devices resemble the conventional thermo-cyclers at their operation; the sample is static in a chamber (well) and both the device and the sample undergo the thermal cycling (Shen et al., 2005). The first type of continuous flow devices which appeared in the literature is the fixed loop devices (Kopp et al., 1998) where the sample moves through fixed temperature zones to achieve the required thermal cycling; the number of cycles is determined at the fabrication stage (Chen et al., 2012). The second type of continuous flow devices is closed loop devices (Bau et al., 2004) where the sample circulates in the temperature zones; the number of thermal cycles can be varied at will during the operation.

The first static chamber μPCR devices had a high thermal mass compared to continuous flow ones: Note that not only the PCR mixture but also the device undergo the thermal cycling. Due to the thermal inertia, the cycling was longer and required higher energy consumption in static chamber devices (Zhang and Ozdemir, 2009). However, the use of flexible polymeric films for the fabrication of μPCR or mixing devices (Moschou et al., 2014; Papadopoulos et al., 2014) and the evolution of the heating elements from external, generally used in thermal cyclers, to integrated, allows reduction in the thermal mass of the static chamber devices and as a consequence rapid heating/cooling rates (Ahmad and Hashsham, 2012). However, a

systematic comparison of continuous flow and static chamber devices in terms of energy consumption is still lacking, especially under the light of flexible substrate devices with integrated microheaters.

The aim of this work is the comparison of a continuous flow vs. a static chamber μPCR device on flexible substrates with integrated microheaters. Comparison is made in terms of energy consumption, speed, and DNA amplification efficiency and is implemented by a computational study. For both devices, the dimensions of the channels as well as the distance of the channels from the integrated heaters are dictated by the material stack and the processes used in flexible printed circuit (FPC) technology (Papadopoulos et al., 2014). Both devices are technologically feasible; the continuous flow device with the integrated heaters has been already fabricated (Moschou et al., 2014).

PCR reaction kinetics is used to calculate DNA amplification; a simple kinetic model is considered and the same protocol is adopted for both devices. The formulation, the estimation of the kinetic parameters, and the implementation of PCR kinetics to evaluate the performance of DNA amplification have been the subject of several previous works (Athavale et al., 2001; Hunicke-Smith, 1997; Li et al., 2012; Mehra and Hu, 2005; Priye et al., 2013; Wang et al., 2007). The contribution of this work in terms of simulation is the detailed (3d) model used for the calculations of the continuous flow μPCR device; it couples fluid flow, species diffusion and PCR reaction kinetics, and heat transfer in both fluid and solid layers of the device. The solution is performed by the finite element method, implemented with COMSOL (COMSOL AB, Sweden).

The rest of the paper is structured as follows: In Sec. 2, the designs of the μPCR devices are presented. In Secs. 3 and 4 the mathematical model and the PCR kinetics are described. In Sec. 5 the simulation results for both the static chamber and continuous flow devices are discussed. The last section summarizes the conclusions.

2. The continuous flow and static chamber devices on flexible polymeric substrates with integrated microheaters

The schematic of the continuous flow device is shown in Fig. 1a; in particular, a part of the device where 3 thermal cycles take place is shown. The design comes from a fabricated device (Moschou et al., 2014): The depth of the meander shaped channel is 50 μm and its width is 200 μm at the denaturation and annealing zones and 400 μm at the extension zone.

The schematic of the static chamber device is shown in Fig. 1b. A chamber lies on top of a microheater. The fluid remains static in the chamber and the microheater provides the desired temperature profile versus time, applying the PCR protocol.

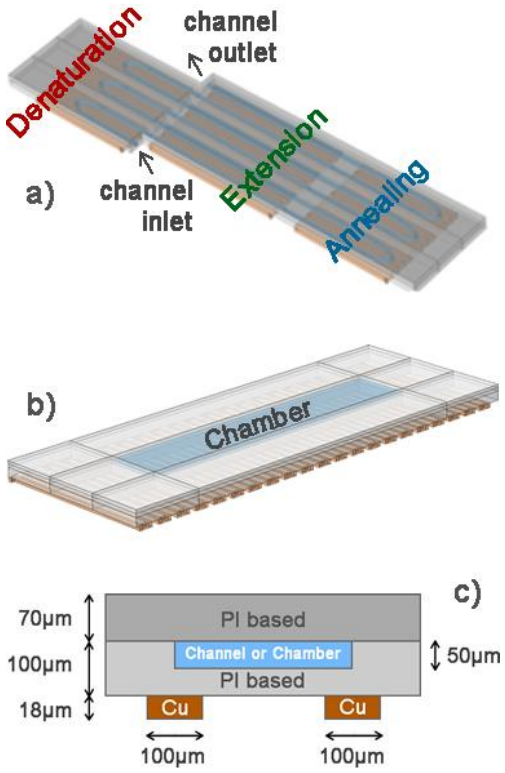

Fig. 1 a) 3 unit cells (3 thermal cycles) of the continuous flow μPCR b) The static chamber μPCR. c) Cross section of the devices, where the material stack is shown.

The material stack for both devices is shown in Fig. 1c and is based on flexible

polymeric films. The device is built on a commercially available Copper-clad polyimide (PI) based substrate (Moschou et al., 2014). The channel is made on the PI-based layer and the meander shaped heaters on the thin (18 μm) Copper (Cu) cladding layer. The sealing layer is also PI-based.

3. Mathematical model

The calculations are performed at the unit cells of both devices, shown in Fig. 2. In the unit cell of the continuous flow device (Fig. 2a), one thermal cycle takes place, whereas at the unit cell of the static chamber device (Fig. 2b), a slice of the whole geometry including one turn of the underlying heater is under study.

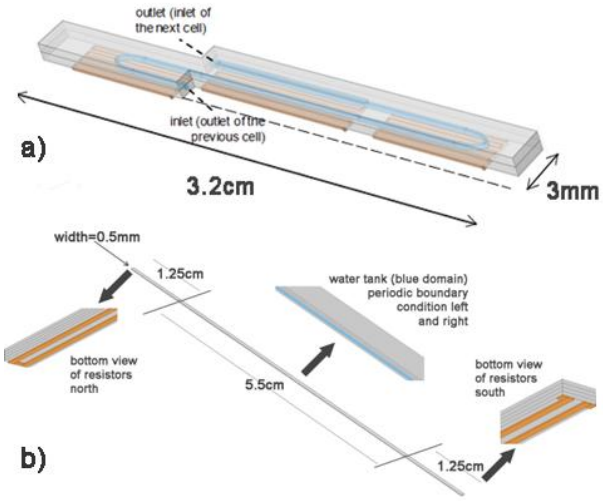

Fig. 2 Unit cells for the numerical calculations in a) the continuous flow and b) the static chamber μPCR devices

The model used for μPCR device simulations consists of the continuity equation

$$\nabla \cdot (\rho \mathbf{u}) = 0 \qquad (1)$$

and the momentum conservation equation

$$\rho(\mathbf{u} \cdot \nabla)\mathbf{u} = \\ = \nabla[-pI + \mu(\nabla \mathbf{u} + (\nabla \mathbf{u})^T) - \frac{2}{3}\mu(\nabla \cdot \mathbf{u})I] \qquad (2)$$

where **u**, ρ, μ, and p are the velocity vector, the density, the dynamic viscosity, and the pressure of the fluid, respectively.

It also includes the mass conservation equation of the species,

$$\nabla \cdot (-D_i \nabla C_i) + \mathbf{u} \cdot \nabla C_i = R_i \qquad (3)$$

where D_i, C_i and R_i are the diffusion coefficient, the concentration, and the net production rate of each species i joining the PCR mixture, e.g. the double-stranded DNA or the primers. The net production rate is defined by the reaction kinetics (see Sec. 4).

The model is complemented by the heat transfer equation in the solid layers and the fluid

$$\rho C_p \cdot \nabla T + \rho C_p \mathbf{u} \cdot \nabla T = \nabla (k \nabla T) + Q \qquad (4)$$

where T, C_p and k are the temperature, the heat capacity, and the thermal conductivity of the layer, respectively. The velocity **u** in Eq. (4) is zero for all domains except for the fluid domain in the continuous flow device. Q is the heat generation rate. This is zero for all domains except for heaters: A different heat generation rate is required at each heater to achieve the desired set point at each zone. The heat generation rates required to keep the set points in the three zones of PCR device are calculated using a binary optimization algorithm developed in Matlab (MathWorks).

No slip condition for the velocity and zero derivatives for the concentration are considered at the walls of the microchannels. Fully developed parabolic profiles of flow are considered at the inlets whereas zero derivatives of both velocity and concentration in the outflow direction are considered at the outlet.

Convection with a heat transfer coefficient h=10W/(m^{2}K) and heat transfer by radiation with surface emissivity ε=0.97 is assumed on all external surfaces. The calculations are performed in a unit cell and periodic heat conditions are applied at the corresponding boundaries. For the continuous flow case, concentration profiles at the outlet of cycle ν are assigned at the inlet of cycle ν+1.

The equations are numerically solved in 3d by the finite element method implemented by COMSOL. For the continuous flow case the equations are solved at steady state. For the static chamber case, the equations are solved in transient state, i.e. an additional transient term is added to the equations.

4. PCR Kinetics

The kinetics for DNA amplification, presented by Hunicke-Smith (Hunicke-Smith, 1997) is considered for both devices. The reaction set for the three steps of PCR, i.e. denaturation (95°C), annealing (55°C), and extension (72°C) is following:

Denaturation

$$S_1\,S_2 \underset{k_D^-}{\overset{k_D^+}{\rightleftarrows}} S_1 + S$$

Annealing

$$S_1 + P_2 \underset{k_A^-}{\overset{k_A^+}{\rightleftarrows}} S_1 P$$

$$S_2 + P_1 \underset{k_A^-}{\overset{k_A^+}{\rightleftarrows}} P_1 S$$

Extension

$$S_1\,P_2 \xrightarrow{k_E} S_1 S$$

$$P_1\,S_2 \xrightarrow{k_E} S_1 S$$

S_1S_2 represents the double-stranded DNA, S_1 and S_2 its single strands, P_1 and P_2 the forward and reverse primers, and S_1P_2 and P_1S_2 the primer-single stranded DNA complexes. Table 1 contains the diffusion coefficients of all species (Wang et al., 2007). The reaction rate constants originate from the functional formulas of Hunicke-Smith (Hunicke-Smith, 1997) and the work of Wang et al. (Wang et al., 2007):

$$k_D^+(T) = \frac{k_0^+\left(1+\tanh\left[\frac{T-88}{5}\right]\right)}{2} \qquad (5)$$

$$k_D^-(T) = \frac{k_0^-\left(1+\tanh\left[\frac{-(T-75)}{5}\right]\right)}{2} \qquad (6)$$

$$k_A^+(T) = \frac{k_1^+\left(1+\tanh\left[\frac{-(T-62.5)}{5}\right]\right)}{2} \qquad (7)$$

$$k_A^-(T) = \frac{k_1^-\left(1+\tanh\left[\frac{T-66}{5}\right]\right)}{2} \qquad (8)$$

$$k_E(T) = k_2 \exp\left(-\left[\frac{T-72}{5}\right]^2\right) \qquad (9)$$

T is the fluid temperature in °C, and k_0^+, k_0^-, k_1^+, k_1^- and k_2 are equal (Wang et al., 2007) to 12.5 s^{-1}, 10^9 $M^{-1}s^{-1}$, 5×10^9 $M^{-1}s^{-1}$, 10^{-4} s^{-1}, and 0.32 s^{-1}, respectively.

Fig. 3 shows the dependence of the reaction rate constants on temperature.

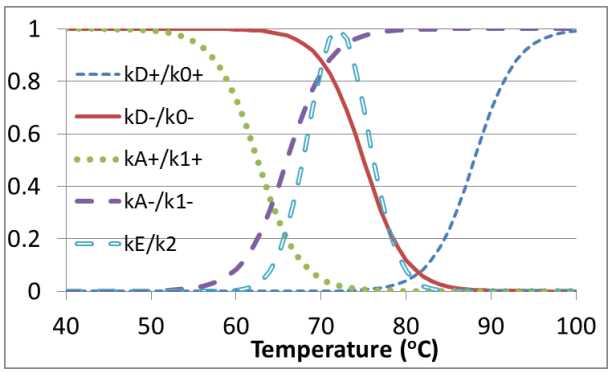

Fig. 3 Normalized reaction rate constants vs. the fluid temperature

Table 1
Initial concentrations and diffusion coefficients of the species of PCR mixture (Wang et al., 2007).

Species	Initial Concentration [mol/m^3]	Diffusion Coefficient [m^2/s]
S_1 & S_2	0	10^{-10}
P_1 & P_2	3×10^{-7}	10^{-9}
S_1P_2 & P_1S_2	0	10^{-10}
S_1S_2	5.71×10^{-12}	10^{-10}

5. Results and discussion

For an objective comparison in terms of energy consumption, required time, and DNA amplification efficiency, the calculations are performed under the following conditions: a) The same stack of materials is considered for both devices (Fig. 1c). b) The PCR samples to be amplified have the same volume of 5.3 μl and the same initial concentrations (Table 1). c) The same PCR kinetics, the same PCR protocol, and the same number of cycles are considered for both devices. The PCR protocol is 4s:5.6s:8.2s (for denaturation, annealing, and extension times, respectively) and is defined by i) the relative ratios of the channel volumes of the continuous flow device and ii) a specification for the DNA sample to flow through 30 cycles in less than 15 min. Even if real PCR processes require 25-35 cycles, to accelerate computations, the comparisons are made for 10 cycles which are enough to extract safe conclusions. Finally, the time required for each device, includes not only the time for the amplification of a 5.3 μl DNA sample, but also the time required for the pumping of the sample in and out of the devices.

5.1 Continuous flow μPCR

The unit cell geometry shown in Fig. 2a is used for the continuous flow μPCR calculations. This unit cell provides a fluid volume of 0.53 μl, i.e. 10 cycles correspond to a total fluid volume of 5.3 μl. The average velocity at the inlet is 2.2 mm/s (which yields into the following PCR protocol 4s:5.6s:8.2s).

For a mesh-independent solution for the velocity, pressure, and temperature [Eqs. (1), (2), and (4)], 2,008,846 elements are required, while 279,632 elements are required for the equations of the species mass conservation [Eq. (3)].

Fig. 4 shows the DNA amplification for 10 cycles. The average DNA concentration at the outlet is found to be ca. 890 times the initial DNA concentration, in good agreement with the ideal 2^{10} (1024x) amplification.

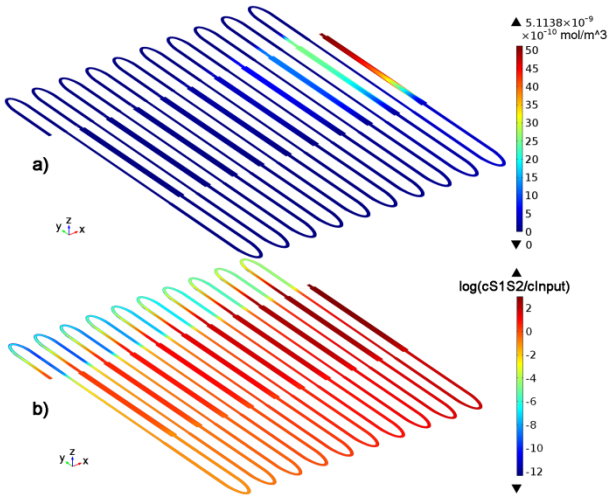

Fig. 4 a) DNA concentration and b) the logarithm of DNA amplification in continuous flow device

The required duration for the amplification of a 5.3 μl sample in a 10 cycle μPCR device is equal to ca. 469 s. This value comes from the multiplication of the time required for 1 cycle [0.53 μl / (volumetric flow rate)] with 20 (10×2). The extra multiplication by 2 takes into account the time required to have a total volume of 5.3 μl amplified.

The total energy consumption is the sum of heat generation rates at the heaters multiplied by the total time required and it is calculated ca. 639 J.

5.2 Static chamber μPCR

The unit cell geometry, shown in Fig. 2b, is used for the static chamber μPCR simulation. The simulation is performed at transient state by solving the heat transfer equation in both the solid and the fluid as well as the mass conservation equations of the diluted species. A mesh independent solution requires 93,988 elements.

The protocol is the same as in the continuous flow μPCR. Instead of time dependent heat generation rate at the heater, experimental data showing the temperature evolution at the heater are used. In particular, the temperature gradients at the heater during the transition from denaturation to annealing, annealing to extension, and extension to denaturation have been measured [Table 2, (Moschou et al., 2014)] in a device realized on the same material stack. The temperature evolution for 10 cycles at the heater is shown

in Fig. 5a; this temperature profile vs. time is used as temperature boundary condition at the heater.

Table 2
Temperature gradients at the heaters of the static chamber PCR device (Moschou et al., 2014)

Zones	Gradients [^{o}C/s]
Denaturation → Annealing	7.2
Annealing → Extension	19.5
Extension → Denaturation	12.5

Taking into account the experimentally measured temperature gradients of the heater, it is found that each cycle lasts 26.15 s. Thus, the total time needed to amplify the initial DNA sample and retrieve the final DNA product is found to be 261.5 s (26.15s×10) plus the time required to pump the DNA sample into and out of the chamber; the latter term is two times the ratio of the total volume of 5.3 μl over the volumetric flow rate used for pumping. If a reasonable volumetric flow rate i.e., 5 μl/min is used, the total time is 389 s.

Fig. 5a shows the average temperature of the DNA sample (fluid) along with the temperature at the heater vs. time for 10 cycles. Fig. 5b shows the temporal variation of the average DNA concentration. The average DNA concentration after 10 cycles is ca. 678 times the initial DNA concentration.

The total power consumption is estimated by the following equation

$$P_{sc} = \iiint \rho C_p \frac{dT}{dt} dV + \\ + \iint h\left(T - T_{amb}\right) dA + \iint \varepsilon\sigma\left(T^4 - T_{amb}^4\right) dA \quad (10)$$

where σ is the Stefan-Boltzmann constant, T_{amb} is the ambient temperature, V is the total volume of the unit cell, and A is the surface of the unit cell which is in contact with the ambient.

The first of the three terms at the right hand side of Eq. (10) is the power absorbed by the volume of the unit cell; it is negative in the period of cooling of the cycle, i.e. during the transition from the denaturation to the annealing temperature. The second and third terms are the heat loss rates to the ambient due to convection (second term) and radiation (third term). The latter heat loss rates are enough to cool the fluid during the cooling period of the cycle. The total power as well as the three terms of the right hand side of Eq. (10) are shown in Fig. 6 versus time for 3 cycles.

The energy required for 10 cycles is calculated by the integration of the power profile over the time of 10 cycles (261.5 s); this time is the net time for amplification and does not include the time for pumping. The total energy consumption for a sample of 5.3 μl is calculated ca. 112 J.

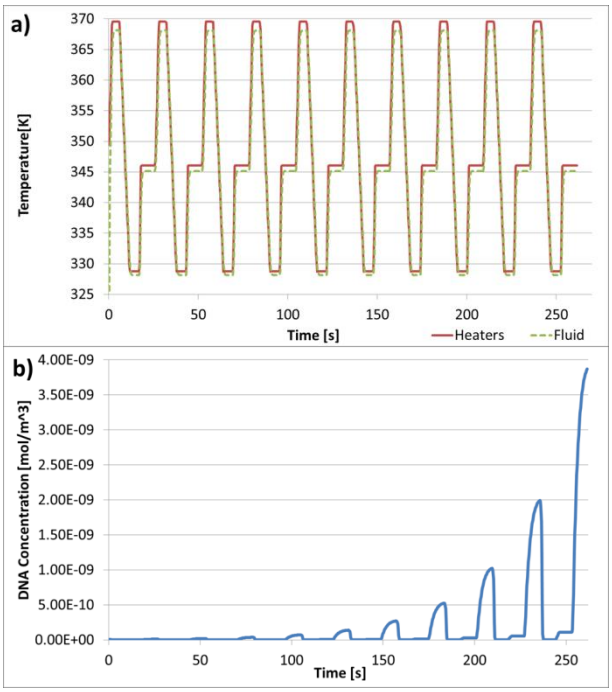

Fig. 5 a) Temperature of the fluid and at the heater vs. time and b) DNA concentration in the static chamber μPCR device.

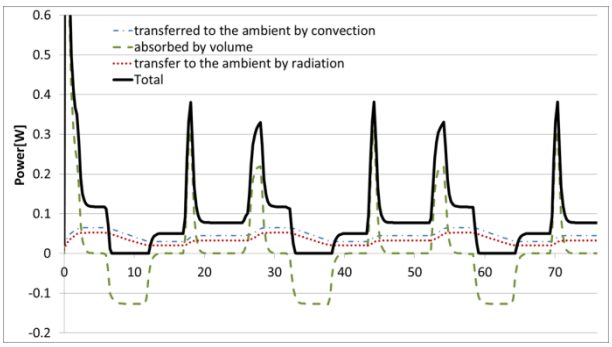

Fig. 6 Total power, power absorbed by the volume of the unit cell, power transferred to the ambient by convection and radiation in the static chamber μPCR device for 3 PCR cycles. The total power needed at t=0 is 1.94 W.

5.3 Comparison

The results of the comparison are summarized in Table 3. A higher degree of DNA amplification is achieved by the continuous flow device. This is due to the inevitable passing of the fluid from an intermediate zone, kept at the extension temperature, while flowing from the denaturation to the annealing zone. In this particular zone, the existence of primer-ssDNA (S_1P_2 and S_2P_1) products that did not react in the extension zones of previous cycles, causes the increase in the concentration of dsDNA.

Table 3
Continuous flow vs. static chamber PCR performance

Type	Continuous Flow	Static Chamber
DNA amplification	890	678
Energy consumption (J)	639	112
10 cycle duration (s)	469	$261.5 + 2\times5.3\ \mu l/\dot{V}$ $389, \dot{V}$ =5 μl/min

The DNA concentration at the end of each cycle for both devices is shown in Fig. 7.

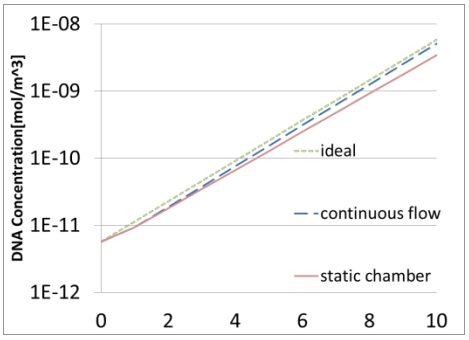

Fig. 7 DNA concentration at the end of each thermal cycle for the continuous flow and the static chamber device; the ideal case, i.e. the case where the DNA concentration multiplies with 2 in every cycle is also shown.

Even if the total time required for the static chamber μPCR device typically depends on the volumetric flow rate for the pumping of the DNA sample into and out of the device, it is at least comparable with the time required for the continuous flow device.

Finally, the energy consumption in the static chamber μPCR is significantly lower compared to the continuous flow μPCR. The latter can be explained by the smaller thermal mass of the static chamber μPCR; a static chamber device carrying 5.3 μl of DNA sample is 32 μl, while a continuous flow device is 132 μl.

6. Conclusions

In this work the performance of two μPCR devices, i.e. a static chamber and continuous flow device, fabricated on flexible substrates with integrated microheaters, is evaluated by simulation. A mathematical model which couples fluid flow, heat transfer in both solid and fluid, mass conservation of species, and PCR reaction kinetics is numerically solved by COMSOL. The case studied is the amplification of 5.3 μl of a DNA sample under a 4s:5.6s:8.2s protocol for 10 cycles. The specifications regarding the material stack is the same for both devices and originates from the FPC technology implemented for the device fabrication.

The results show that continuous flow device has an advantage with respect to DNA amplification efficiency, being closer to the ideal amplification (Table 3). However, the continuous flow device requires (~ 6 times) greater energy consumption compared to the static chamber device which is justified by the smaller thermal mass of the static chamber device. Finally, the total times required for both devices are comparable.

The calculations under the conditions of this work show that, despite the consensus in favor of continuous flow devices, static chamber μPCR devices fabricated on flexible substrates with integrated microheaters can be better compared to their counterpart continuous flow μPCR devices; this superiority is crearly the outcome of using flexible polymeric films with integrated microheaters; the thermal mass has been greatly reduced compared to the conventional thermal cyclers or the first generation of microfabricated static μPCR devices. Along

with this advantage, comes the flexibility of a static chamber device to serve any PCR protocol; continous flow devices serve only a specific number of protocols defined by the relative volume ratios of the dentaturation :annealing:extension microchannels. Both the low energy consumpion and the flexibility indicate attractive prospects for static chamber μPCR devices realized on flexible substrates with integrated microheaters.

Acknowledgements

This work is partly supported by the EU project (FP7-ICT-2011.3.2) LOVE-FOOD: Love wave fully integrated Lab-on-Chip platform for food pathogen detection (Grant agreement no: 317742)

References

Ahmad, F., Hashsham, S.A., 2012. Miniaturized nucleic acid amplification systems for rapid and point-of-care diagnostics: a review. Analytica chimica acta 733, 1-15.

Athavale, M., Chen, Z., Furmanczyk, M., Przekwas, A., 2001. Coupled multiphysics and chemistry simulations of PCR microreactors with active control, Proc. Int. Conf. Modeling and Simulation of Microsystems, pp. 574-577.

Bau, H.H., Chen, Z.Y., Qian, S.Z., Abrams, W.R., Malamud, D., 2004. Thermosiphon-based PCR reactor: Experiment and modeling. Analytical Chemistry 76, 3707-3715.

Chen, P.-C., Fan, W., Hoo, T.-K., Chan, L.C.Z., Wang, Z., 2012. Simulation guided-design of a microfluidic thermal reactor for polymerase chain reaction. Chemical Engineering Research and Design 90, 591-599.

Hunicke-Smith, S.P., 1997. PCR and cycle sequencing reactions: a new device and engineering model. PhD Thesis, Department of Mechanical Engineering, Stanford University, pp. 104, 109-110.

Kopp, M.U., de Mello, A.J., Manz, A., 1998. Chemical amplification: Continuous-flow PCR on a chip. Science 280, 1046-1048.

Kumar, S., Thorsen, T., Das, S.K., 2008. Thermal modeling for design optimization of a microfluidic device for continuous flow polymerase chain reaction (PCR), ASME 2008 Heat Transfer Summer Conference collocated with the Fluids Engineering, Energy Sustainability, and 3rd Energy Nanotechnology Conferences. American Society of Mechanical Engineers, pp. 323-330.

Li, L., Wang, C., Song, B., Mi, L., Hu, J., 2012. Kinetic Parameters Estimation in the Polymerase Chain Reaction Process Using the Genetic Algorithm. Industrial & Engineering Chemistry Research 51, 13268-13273.

Mehra, S., Hu, W.-S., 2005. A kinetic model of quantitative real-time polymerase chain reaction. Biotechnology and Bioengineering 91, 848-860.

Moschou, D., Vourdas, N., Kokkoris, G., Papadakis, G., Parthenios, J., Chatzandroulis, S., Tserepi, A., 2014. All-plastic, low-power, disposable, continuous-flow PCR chip with integrated microheaters for rapid DNA amplification. Sensors & Actuators: B. Chemical 199, 470–478.

Papadopoulos, V.E., Kefala, I.N., Kaprou, G., Kokkoris, G., Moschou, D., Papadakis, G., Gizeli, E., Tserepi, A., 2014. A passive micromixer for enzymatic digestion of DNA. Microelectronic Engineering 124, 42–46.

Priye, A., Hassan, Y.A., Ugaz, V.M., 2013. Microscale Chaotic Advection Enables Robust Convective DNA Replication. Analytical Chemistry 85, 10536-10541.

Shen, K., Chen, X., Guo, M., Cheng, J., 2005. A microchip-based PCR device using flexible printed circuit technology. Sensors and Actuators B: Chemical 105, 251-258.

Wang, Y., Pant, K., Grover, J., Sundaram, S., 2007. Multi-physics Simulational Analysis of a Novel PCR Micro-Device. Nanotech 3, 456-459.

Zhang, Y., Ozdemir, P., 2009. Microfluidic DNA amplification--a review. Analytica chimica acta 638, 115-125.